

## Measurement of antiproton annihilation on Cu, Ag and Au with emulsion films

---

S. Aghion<sup>a,b</sup>, C. Amsler<sup>c,d</sup>, A. Ariga<sup>c</sup>, T. Ariga<sup>c\*</sup>, G. Bonomi<sup>e,f</sup>, P. Bräunig<sup>g</sup>, R. S. Brusa<sup>h,i</sup>, L. Cabaret<sup>j</sup>, M. Caccia<sup>b,k</sup>, R. Caravita<sup>l,m</sup>, F. Castelli<sup>b,n</sup>, G. Cerchiari<sup>o</sup>, D. Comparat<sup>i</sup>, G. Consolati<sup>a,b</sup>, A. Demetrio<sup>g</sup>, L. Di Noto<sup>l,m</sup>, M. Doser<sup>p</sup>, A. Ereditato<sup>c</sup>, C. Evans<sup>a,b</sup>, R. Ferragut<sup>a,b</sup>, J. Fesel<sup>p</sup>, A. Fontana<sup>f</sup>, S. Gerber<sup>p</sup>, M. Giammarchi<sup>i</sup>, A. Gligorova<sup>q</sup>, F. Guatieri<sup>h,i</sup>, S. Haider<sup>p</sup>, H. Holmestad<sup>r</sup>, T. Huse<sup>r</sup>, J. Kawada<sup>c</sup>, A. Kellerbauer<sup>o</sup>, M. Kimura<sup>c</sup>, D. Krasnický<sup>l,m</sup>, V. Lagomarsino<sup>l,m</sup>, P. Lansonneur<sup>s</sup>, P. Lebrun<sup>s</sup>, C. Malbrunot<sup>d,p</sup>, S. Mariazzi<sup>d</sup>, V. Matveev<sup>t,u</sup>, Z. Mazzotta<sup>b,n</sup>, G. Nebbia<sup>v</sup>, P. Nedelec<sup>s</sup>, M. Oberthaler<sup>g</sup>, N. Pacifico<sup>q</sup>, D. Pagano<sup>e,f</sup>, L. Penasa<sup>h,i</sup>, V. Petracek<sup>w</sup>, C. Pistillo<sup>c</sup>, F. Preiz<sup>b</sup>, M. Prevedelli<sup>x</sup>, L. Ravelli<sup>h,i</sup>, B. Rienaecker<sup>p</sup>, O. M. Røhne<sup>r</sup>, A. Rotondi<sup>f,y</sup>, M. Sacerdoti<sup>b,n</sup>, H. Sandaker<sup>r</sup>, R. Santoro<sup>b,k</sup>, P. Scampoli<sup>e,z</sup>, M. Simon<sup>d</sup>, L. Smestad<sup>p,aa</sup>, F. Sorrentino<sup>l,m</sup>, G. Testera<sup>m</sup>, I. C. Tietje<sup>p</sup>, S. Vamosi<sup>d</sup>, M. Vladymyrov<sup>c</sup>, E. Widmann<sup>d</sup>, P. Yzombard<sup>j</sup>, C. Zimmer<sup>o,p</sup>, J. Zmeskal<sup>d</sup>, N. Zurlo<sup>f,bb</sup>

- <sup>a</sup>Politecnico di Milano, Piazza Leonardo da Vinci 32, 20133 Milano, Italy
- <sup>b</sup>INFN Milano, via Celoria 16, 20133, Milano, Italy
- <sup>c</sup>Laboratory for High Energy Physics, Albert Einstein Center for Fundamental Physics, University of Bern, 3012 Bern, Switzerland
- <sup>d</sup>Stefan Meyer Institute for Subatomic Physics, Austrian Academy of Sciences, Boltzmannngasse 3, 1090 Vienna, Austria
- <sup>e</sup>Department of Mechanical and Industrial Engineering, University of Brescia, via Branze 38, 25123 Brescia, Italy
- <sup>f</sup>INFN Pavia, via Bassi 6, 27100 Pavia, Italy
- <sup>g</sup>Kirchhoff-Institute for Physics, Heidelberg University, Im Neuenheimer Feld 227, 69120 Heidelberg, Germany
- <sup>h</sup>Department of Physics, University of Trento, via Sommarive 14, 38123 Povo, Trento, Italy
- <sup>i</sup>TIFPA/INFN Trento, via Sommarive 14, 38123 Povo, Trento, Italy
- <sup>j</sup>Laboratoire Aimé Cotton, Université Paris-Sud, ENS Cachan, CNRS, Université Paris-Saclay, 91405 Orsay Cedex, France
- <sup>k</sup>Department of Science, University of Insubria, Via Valleggio 11, 22100 Como, Italy
- <sup>l</sup>Department of Physics, University of Genova, via Dodecaneso 33, 16146 Genova, Italy
- <sup>m</sup>INFN Genova, via Dodecaneso 33, 16146 Genova, Italy
- <sup>n</sup>Department of Physics, University of Milano, via Celoria 16, 20133 Milano, Italy
- <sup>o</sup>Max Planck Institute for Nuclear Physics, Saupfercheckweg 1, 69117 Heidelberg, Germany
- <sup>p</sup>Physics Department, CERN, 1211 Geneva 23, Switzerland
- <sup>q</sup>Institute of Physics and Technology, University of Bergen, Allégaten 55, 5007 Bergen, Norway
- <sup>r</sup>Department of Physics, University of Oslo, Sem Sælands vei 24, 0371 Oslo, Norway
- <sup>s</sup>Institute of Nuclear Physics, CNRS/IN2p3, University of Lyon 1, 69622 Villeurbanne, France
- <sup>t</sup>Institute for Nuclear Research of the Russian Academy of Science, Moscow 117312, Russia
- <sup>u</sup>Joint Institute for Nuclear Research, 141980 Dubna, Russia
- <sup>v</sup>INFN Padova, via Marzolo 8, 35131 Padova, Italy
- <sup>w</sup>Czech Technical University, Prague, Brehová 7, 11519 Prague 1, Czech Republic
- <sup>x</sup>University of Bologna, Viale Berti Pichat 6/2, 40126 Bologna, Italy
- <sup>y</sup>Department of Physics, University of Pavia, via Bassi 6, 27100 Pavia, Italy
- <sup>z</sup>Department of Physics “Ettore Pancini”, University of Napoli Federico II, Complesso Universitario di Monte S. Angelo, 80126, Napoli, Italy
- <sup>aa</sup>The Research Council of Norway, P.O. Box 564, NO-1327 Lysaker, Norway
- <sup>bb</sup>Department of Civil Engineering, University of Brescia, via Branze 43, 25123 Brescia, Italy

*E-mail:* tomoko.ariga@lhcp.unibe.ch

**ABSTRACT:** The characteristics of the process of low energy antiproton annihilation on nuclei (e.g. hadronization and product multiplicities) are not well known, and Monte Carlo simulation packages that use different models provide different descriptions of the annihilation events. In this study, we measured the particle multiplicities resulting from antiproton annihilations on nuclei. The results were compared with predictions obtained using different models in simulation tools such as GEANT4 and FLUKA. For this study, we exposed thin targets (Cu, Ag and Au) to a very low energy antiproton beam from CERN's antiproton decelerator, exploiting the secondary beam-line available in the AEgIS (AD6) experimental zone. The antiproton annihilation products were detected using emulsion films developed at the Laboratory of High Energy Physics in Bern where they were analysed at the automatic microscope facility. The fragment multiplicity measured in this study is in good agreement with results obtained with FLUKA simulations for both minimally and heavily ionizing particles.

**KEYWORDS:** Particle detectors; Emulsion detectors; Antiproton annihilations.

---

\*Corresponding author.

---

## Contents

<b>1. Introduction</b>	<b>1</b>
<b>2. Experimental setup</b>	<b>2</b>
<b>3. Data analysis and results</b>	<b>2</b>
<b>4. Conclusions</b>	<b>8</b>

---

## 1. Introduction

Emulsion films have recently been considered as possible position detectors for low energy anti-matter studies. These studies include the AEGIS experiment at CERN [1, 2, 3, 4] whose goal is the measurement of the Earth's gravitational acceleration on antihydrogen atoms. Another collaboration proposed emulsions for their studies on positrons, as described in [5]. In particular, in the case of the AEGIS experiment, the position detector must have a micrometer level resolution to allow the required sensitivity of  $\sim 1\%$  to be obtained for the gravitational acceleration measurement. Therefore, the excellent intrinsic spatial resolution of the emulsion detectors [6] has been exploited since they are capable of reconstructing the antihydrogen impact points from the annihilation products. Emulsion films were tested and they exhibited a spatial resolution of  $\sim 1-2 \mu\text{m}$  [3]. Films with this resolution combined with a time of flight detector, could allow the experiment goal to be achieved. In the same paper [3], a preliminary study of antiproton-nuclei annihilations was also reported. That study assessed particle multiplicities resulting from antiproton annihilations on emulsion films and aluminium. Recently, again using the framework of the AEGIS experiment, analogous measurements were performed by means of a silicon detector acting at the same time as an annihilation target [7]. Apart from the obvious applications in nuclear physics, measurement of the decay products of low energy antiproton annihilation in different materials provides a useful check of the ability of standard Monte Carlo packages to reproduce fragment multiplicities, type and energy distributions stemming from antiproton (or antineutron) annihilation at rest on nuclei. In fact, although measurements of the multiplicities of pions and other charged particles with energies higher than approximately 50 MeV are available in the literature [8, 9], the production of highly ionizing nuclear fragments with short range has not been sufficiently studied. A measurement of the multiplicities of charged products in antiproton-aluminium annihilations was reported in [3], although the statistics performed in this study were 43 events, and the tracking efficiency of the detector was limited to 80%. In this paper, we present the results of a study of the multiplicities of charged annihilation products on different target materials, namely copper, silver and gold, using emulsion detectors at the Antiproton Decelerator (AD) at CERN.

## 2. Experimental setup

Emulsion detectors were used to study the antiproton annihilation products generated in different materials. This was conducted using a secondary beam line located in the AEGIS zone at the AD. Before reaching the targets, the 5.3 MeV antiprotons from the AD ( $3 \times 10^7$  pbar/shot every 100 s) were moderated in successive steps by means of different titanium and aluminium foils with variable thicknesses. Finally, the beam was collimated in a vacuum test chamber after crossing a vacuum separation window of titanium with a thickness of  $12 \mu\text{m}$ . The emulsion detector was situated at the downstream end of the vacuum chamber ( $\sim 1$  m in length) where it could be reached by a defocused beam of low energy antiprotons ( $\sim 100$  keV). This distance from the degrading layer was necessary to reduce the background from annihilations taking place at the moderator. A sketch of the experimental setup is shown in Fig. 1. The emulsion detector was operated under ordinary vacuum conditions ( $10^{-5} - 10^{-6}$  mbar). The antiproton intensity measured by the detector was approximately  $150/\text{cm}^2/\text{shot}$ .

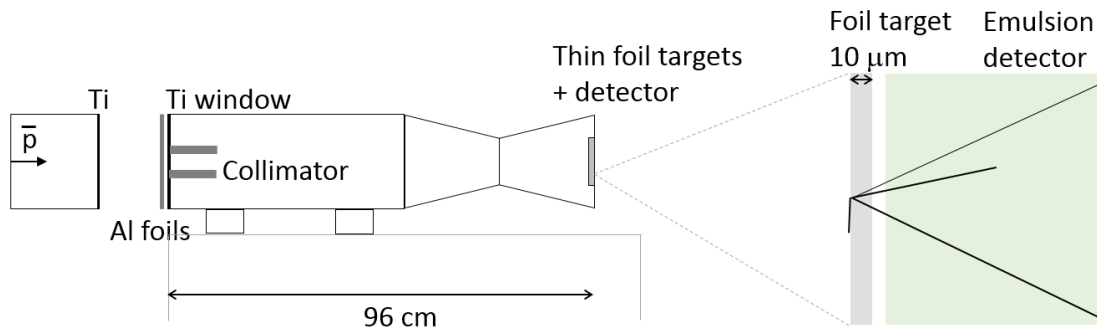


**Figure 1.** Schematic setup of the experiment. An enlarged view of the target region is shown on the right side.

For this study the emulsion detectors (for a review on the emulsion technology see [6]) were produced at the Laboratory for High Energy Physics (LHEP) of the University of Bern by pouring the emulsion gel, provided by Nagoya University (Japan), on a glass plate. Glycerin was added to the emulsion gel so that it could operate in vacuum [3]. This emulsion features a very low background with a number of thermally induced grains of approximately 1-2 grains/ $1000 \mu\text{m}^3$  [5].

Foils of copper, silver and gold, each having a thickness of  $10 \mu\text{m}$ , were placed as targets at the end of the vacuum chamber, in front of the emulsion detectors (one setup with copper and silver and the other one with gold). With these setups and given the antiproton energies, all the annihilations are expected to take place within a few  $\mu\text{m}$  of the surface. Fig. 2 shows the targets ( $2 \times 2 \text{ cm}^2$ ) fixed to the emulsion film (left and middle) and an antiproton annihilation taking place directly on the emulsion surface (right). During data taking, we collected approximately  $1500$  antiprotons per  $\text{cm}^2$  in about 10 AD shots.

## 3. Data analysis and results

Data recorded by the emulsion detectors were automatically scanned by an optical microscope

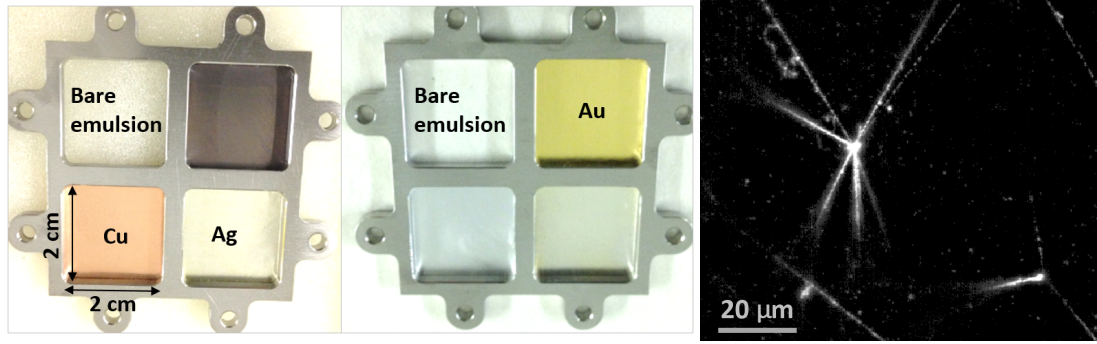


**Figure 2.** Left and middle: Target arrangement in the two setups, fixed to the emulsion films. Targets other than Cu, Ag and Au were not included in our study. Right: Antiproton annihilations on the bare emulsion surface.

and then analysed by exploiting a recently developed fast tracking algorithm [10]. The measured tracking efficiency of our detector was approximately 99% for minimally ionizing particles for a wide angular range as reported in [10].

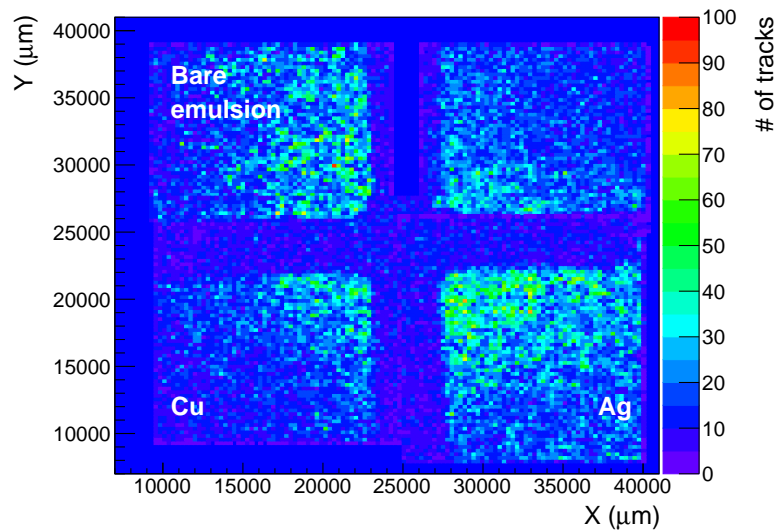


**Figure 3.** Profile of detected tracks (XY positions of tracks at the emulsion layer) in one of the setups. The top right part was not included in our study.

Fig. 3 shows the profile of detected tracks (XY positions of tracks at the emulsion layer) in one of the setups. Among the tracks reconstructed by the above algorithm, we only considered those tracks that were longer than  $30 \mu\text{m}$  and in the direction of the antiproton beam to avoid considering tracks that were due to the background. An angular cut of  $0.4 < \tan\theta < 2.0$  ( $22^\circ < \theta < 63^\circ$ ), with  $\theta$  representing the track angle with respect to the beam direction, was applied. To reconstruct a vertex, two three-dimensional tracks were required. The efficiency of vertex finding was estimated by applying the criteria given above to the output of the FLUKA simulation and was found to be 22% for copper, 24% for silver, and 18% for gold.

The position of the reconstructed annihilation vertices can be used to calculate the magnitude of the actual gap between the emulsion film and metal foils, which in principle were put in contact with the detector. The surface topography obtained from the reconstructed vertices is shown in Fig. 4 for copper, silver and gold targets. In our analysis, we only considered regions less than  $100 \mu\text{m}$  from the emulsion film surface because the vertex finding efficiency was uniform within a few percent. The analysed fiducial area was  $1.68 \text{ cm}^2$  for the copper target,  $1.96 \text{ cm}^2$  for silver and  $0.80 \text{ cm}^2$  for gold.

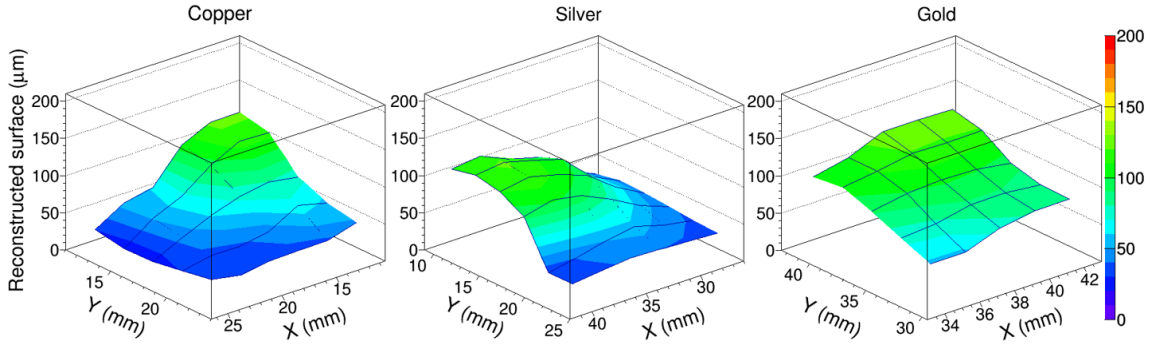


**Figure 4.** Surface topography for copper, silver and gold targets obtained from the reconstructed vertices. The vertical scale refers to the distance from the emulsion film. The precision of target foil position is approximately  $14 \mu\text{m}$  in the vertical direction.

The main source of the background signal in the reconstructed vertices was due to accidental coincidences of tracks coming from annihilations taking place upstream in the apparatus, which were not completely excluded by the angular cut due to broad angular distribution. The number of background tracks was much larger than the number of signal tracks, while the signal fraction became significant if vertex reconstruction at the position of the target foil was required. The rate of background vertices was estimated by randomizing the track positions in the analysed area (keeping the slope information constant), reconstructing the vertices and counting the number of vertices that mimicked annihilations in the target.

The estimated background, which depends on the number of prongs in the event, is shown on the left side of Fig. 5, while the right side shows the multiplicity distributions after subtraction of the background, compared with the Monte Carlo predictions based on the CHIPS [11] and FTFP (FTFP\_BERT\_TRV) [12] models in the GEANT4 (4.9.5.p02) and FLUKA (2011.2c) [13] frameworks. A total of 617 signal annihilation vertices were reconstructed for copper, 882 for silver and 219 for gold.

We could also discriminate between heavily ionizing particles (HIPs) such as protons and nuclear fragments and minimally ionizing particles (MIPs), namely pions. Continuous dense tracks corresponded to HIPs, while faint tracks are produced by MIPs, since the aligned grains of these last tracks are separated. The local energy deposition ( $dE/dx$ ) of each track can then be assessed in terms of signal density (S.D.) along the reconstructed tracks using,

$$S.D. = \sum_{x,y,z \in C} S_{xyz}/L.$$

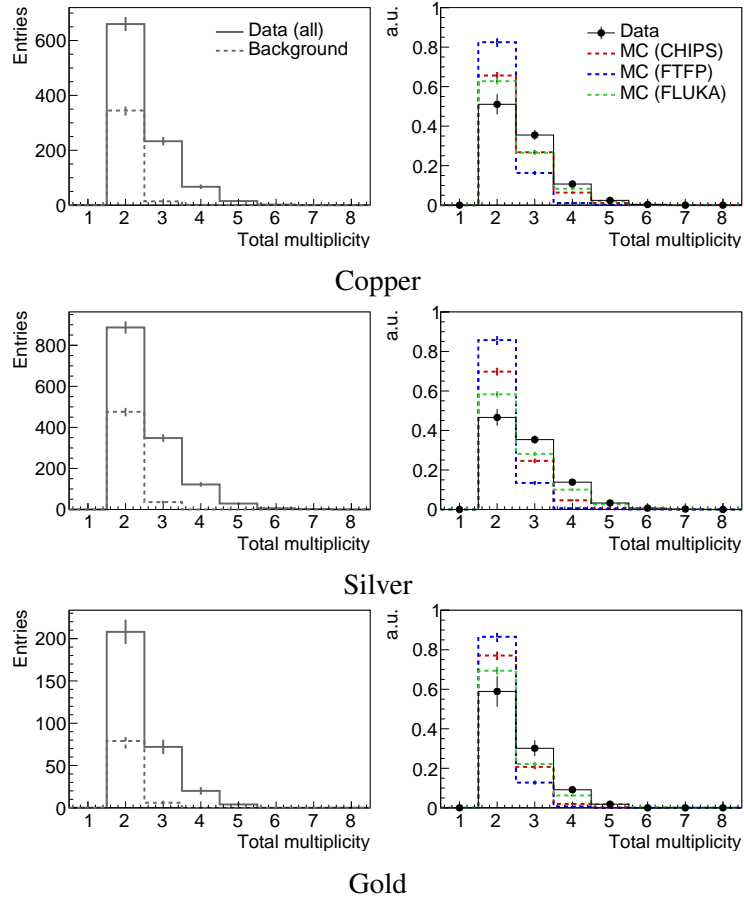


**Figure 5.** Left: Background contributions to the total multiplicities for the different targets. Right: Multiplicity distributions after subtraction of the background. The histograms show the Monte Carlo predictions.

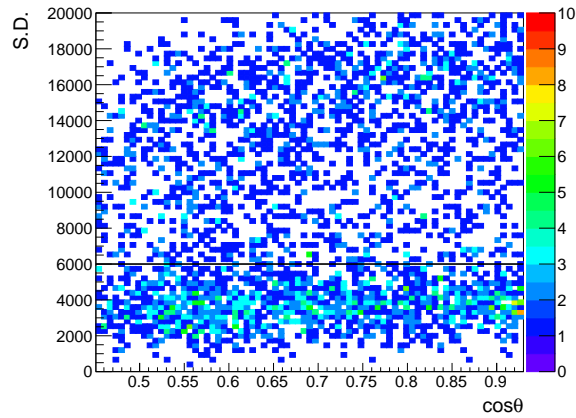


**Figure 6.** Signal density (S.D.) distribution vs track angle with respect to the beam direction. Tracks below the black line are defined as being minimally ionizing.

Here,  $x$ ,  $y$  and  $z$  are the coordinates of voxels in the 3D image data.  $C$  is a group of voxels in a cylinder along the track, and  $S_{xyz}$  is an 8-bit grey-scale signal of the voxel.  $L$  is the length of a

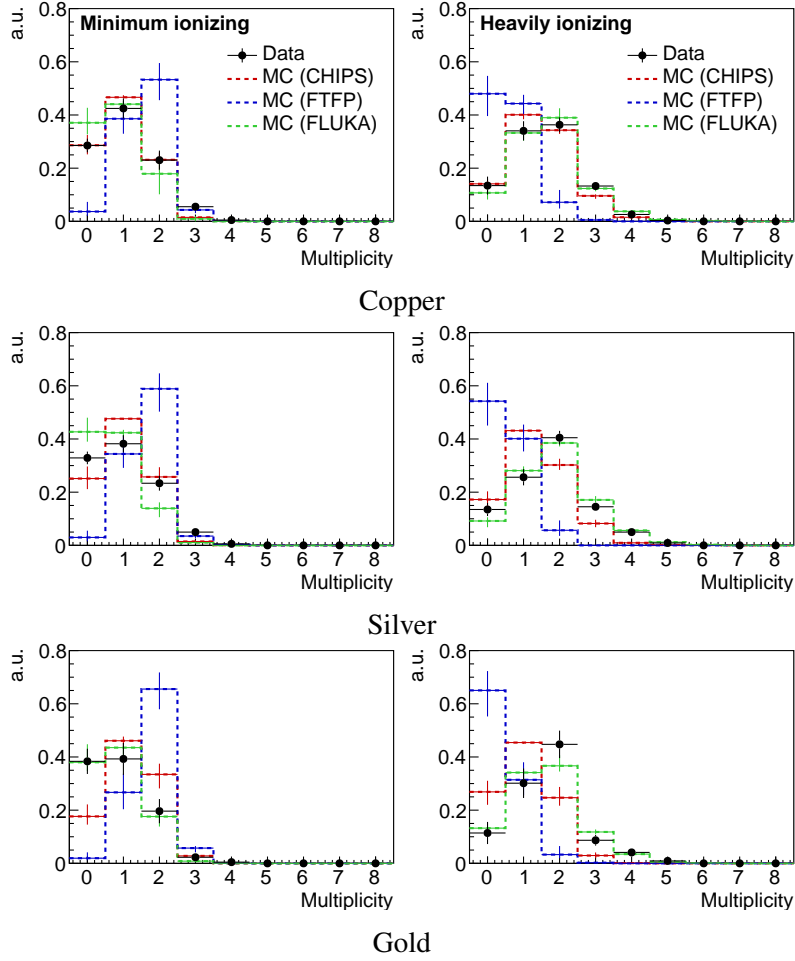


**Figure 7.** Reconstructed multiplicity distributions for annihilations in the copper, silver and gold foils for MIPs (left) and HIPs (right). The histograms show the Monte Carlo predictions by CHIPS, FTFP and FLUKA. The error bars on the histograms account for uncertainties in the  $dE/dx$  classification.

	Average multiplicity for MIPs				Average multiplicity for HIPs			
	Data	CHIPS	FTFP	FLUKA	Data	CHIPS	FTFP	FLUKA
Copper	$1.07 \pm 0.05$	$0.98^{+0.07}_{-0.09}$	$1.59^{+0.09}_{-0.14}$	$0.83^{+0.08}_{-0.11}$	$1.59 \pm 0.06$	$1.46^{+0.09}_{-0.07}$	$0.60^{+0.14}_{-0.10}$	$1.68^{+0.11}_{-0.08}$
Silver	$1.02 \pm 0.04$	$1.04^{+0.08}_{-0.09}$	$1.64^{+0.09}_{-0.13}$	$0.73^{+0.07}_{-0.09}$	$1.75 \pm 0.05$	$1.33^{+0.09}_{-0.08}$	$0.51^{+0.14}_{-0.09}$	$1.87^{+0.09}_{-0.07}$
Gold	$0.87 \pm 0.08$	$1.21^{+0.10}_{-0.11}$	$1.75^{+0.09}_{-0.13}$	$0.81^{+0.07}_{-0.11}$	$1.67 \pm 0.09$	$1.04^{+0.11}_{-0.09}$	$0.39^{+0.13}_{-0.09}$	$1.60^{+0.11}_{-0.06}$

**Table 1.** Measured average multiplicity and Monte Carlo predictions by CHIPS, FTFP and FLUKA. Statistical errors are reported for each set of data. The errors in the predictions account for uncertainties in  $dE/dx$  classification.

reconstructed track in the 3D image data. The S.D. is proportional to the  $dE/dx$  of the particle and does not depend on the angle. However, there is a saturation effect for higher  $dE/dx$  regions. Fig. 6 shows that the S.D. distribution of tracks revealed a peak at 3000 for MIPs. As the simulated  $dE/dx$  distribution of MIPs peaked at  $1.2 \text{ MeV} \cdot \text{g} \cdot \text{cm}^{-2}$ , we define particles with  $dE/dx$  smaller than 2.4

$\text{MeV}\cdot\text{g}\cdot\text{cm}^{-2}$ , corresponding to an S.D. below  $6000\ \mu\text{m}^{-1}$ , as being MIPs. The complementary ones are defined as HIPs.

Fig. 7 shows the track multiplicity distributions for MIPs and HIPs. The errors on the data are statistical. The histograms represent the Monte Carlo predictions by CHIPS, FTFP and FLUKA. The error bars on the Monte Carlo predictions account for uncertainties in the  $dE/dx$  classification. These uncertainties were estimated using simulations, which smeared the threshold for assigning tracks to either class of ionizing particles by 20% and checked for effects on the multiplicity distributions for MIPs and HIPs. The statistical errors for the simulations were 0.01-0.02, which are significantly smaller than the errors reported above. The average multiplicities that were measured are summarized in Table 1. Both CHIPS and FLUKA were in good agreement for copper, particularly in the case of MIPs. Neither CHIPS nor FTFP accurately describe particle multiplicity for annihilations on silver and gold nuclei, while FLUKA seems closer to the data than the other models.

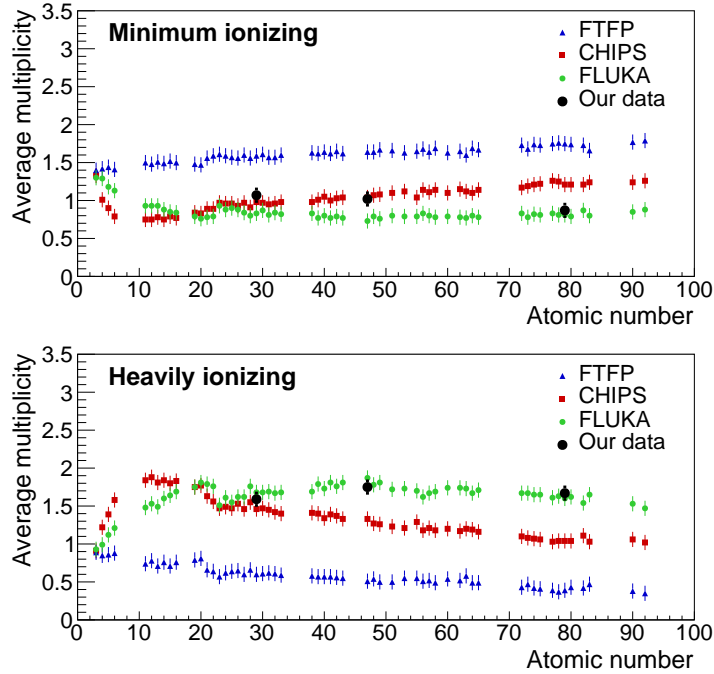


**Figure 8.** Particle multiplicity from antiproton annihilations as a function of atomic number for MIPs (top) and HIPs (bottom).

The mean values of particle multiplicity measured for the three target materials are shown in Fig. 8 as a function of atomic number along with the simulation outcome. Results obtained for MIPs with the FTFP model do not agree with our experimental data for any material, while those obtained with both CHIPS and FLUKA are in close agreement as far as copper is concerned, although only FLUKA reproduces the higher atomic number behaviour. Good agreement with CHIPS was also found for annihilation on bare emulsions and for aluminium [3]. Multiplicity related to HIPs is well described by the FLUKA simulation, while the CHIPS and FTFP models clearly underestimate the number of particles produced by antiproton annihilation.

## 4. Conclusions

The goal of the study presented in this paper was to measure the products of low energy antiproton annihilation on different materials, utilizing a secondary beam line of CERN's antiproton decelerator in the AEGIS experimental area. In fact, the characteristics (e.g. hadronization and fragmentation multiplicities) of low energy antiprotons annihilating on nuclei are not well known and experimental data are needed to validate models used by simulation packages such as GEANT4 and FLUKA. We exposed several thin targets (Cu, Ag and Au) to the antiproton beam and fragment tracks were measured using emulsion detectors with a position resolution at the level of few micrometers, which allowed the separation between minimally and highly ionizing particles. The fragment multiplicity we measured was not well reproduced by the different models used in Monte Carlo simulation with the exception of FLUKA, which seems in good agreement with the particle multiplicity for both minimally and heavily ionizing particles. Future measurements with more materials would be needed to have a better understanding of antinucleon annihilations also on low-Z materials, and to obtain a full description in terms of particle types, multiplicities, as well as in energy, for a more complete benchmarking of Monte Carlo simulations.

## Acknowledgments

This work was supported by the Swiss National Science Foundation Ambizione grant PZ00P2\_154833; Istituto Nazionale di Fisica Nucleare; a Deutsche Forschungsgemeinschaft research grant; an excellence initiative of Heidelberg University; European Research Council under the European Unions Seventh Framework Program FP7/2007-2013 (Grants No. 291242 and No. 277762); Austrian Ministry for Science, Research, and Economy; Research Council of Norway; Bergen Research Foundation; John Templeton Foundation; Ministry of Education and Science of the Russian Federation and Russian Academy of Sciences; and the European Social Fund within the framework of realizing the project, in support of intersectoral mobility and quality enhancement of research teams at Czech Technical University in Prague (Grant No. CZ.1.07/2.3.00/30.0034). The authors would like to acknowledge the contributions by the mechanical workshop at LHEP.

## References

- [1] M. Doser et al., *Exploring the WEP with a pulsed cold beam of antihydrogen*, *Class. Quant. Grav.* **29** (2012) 184009.
- [2] C. Amsler et al., *A new application of emulsions to measure the gravitational force on antihydrogen*, 2013 *JINST* **8** P02015.
- [3] S. Aghion et al. (AEGIS Collaboration), *Prospects for measuring the gravitational free-fall of antihydrogen with emulsion detectors*, 2013 *JINST* **8** P08013.
- [4] S. Aghion et al. (AEGIS Collaboration), *A moiré deflectometer for antimatter*, *Nature Communications* **5** (2014) 4538.
- [5] S. Aghion et al., *Emulsion films for low energy antimatter detection*, 2016 *JINST* **11** P06017.

- [6] A. Ereditato, *The Study of Neutrino Oscillations with Emulsion Detectors*, *Adv. High Energy Phys.* **2013** (2013) 382172.
- [7] S. Aghion et al. (AEgIS Collaboration), *Detection of low energy antiproton annihilations in a segmented silicon detector*, 2014 *JINST* **9** P06020.
- [8] G. Bendiscioli and D. Kharzeev, *Antinucleon-nucleon and antinucleon-nucleus interaction. A review of experimental data*, *Riv. Nuovo Cim.* **17N6** (1994) 1-142.
- [9] D. Polster et al., *Light particle emission induced by stopped anti-protons in nuclei: Energy dissipation and neutron to proton ratio*, *Phys. Rev. C* **51** (1995) 1167-1180.
- [10] A. Ariga and T. Ariga, *Fast  $4\pi$  track reconstruction in nuclear emulsion detectors based on GPU technology*, 2014 *JINST* **9** P04002.
- [11] P.V. Degtyarenko, M. Kosov and H. Wellisch, *Chiral invariant phase space event generator. I: Nucleon antinucleon annihilation at rest*, *Eur. Phys. J. A* **8** (2000) 217; *Chiral invariant phase space event generator. II: Nuclear pion capture at rest and photonuclear reactions below the Delta(3,3) resonance*, *Eur. Phys. J. A* **9** (2000) 411; *Chiral invariant phase space event generator. III: Modeling of real and virtual photon interactions with nuclei below pion production threshold*, *Eur. Phys. J. A* **9** (2000) 421; M. Kossov, *Simulation of antiproton-nuclear annihilation at rest*, *IEEE Trans. Nucl. Sci.* **52** (2005) 2832.
- [12] B. Andersson, G. Gustafson and B. Nilsson-Almqvist, *A model for low- $pT$  hadronic reactions with generalizations to hadron-nucleus and nucleus-nucleus collisions*, *Nucl. Phys. B* **281** (1987) 289; B. Nilsson-Almqvist and E. Stenlund, *Interactions between hadrons and nuclei: The Lund Monte Carlo - FRITIOF version 1.6 -*, *Comput. Phys. Commun.* **43** (1987) 387.
- [13] A. Ferrari, P.R. Sala, A. Fasso, and J. Ranft, *FLUKA: a multi-particle transport code*, CERN 2005-10 (2005), INFN/TC\_05/11, SLAC-R-773; T.T. Bohlen, F. Cerutti, M.P.W. Chin, A. Fasso, A. Ferrari, P.G. Ortega, A. Mairani, P.R. Sala, G. Smirnov, and V. Vlachoudis, *The FLUKA Code: Developments and Challenges for High Energy and Medical Applications*, *Nuclear Data Sheets* **120** (2014) 211-214.